Characterization of Porous Phosphate Coatings Enriched with Calcium, Magnesium, Zinc and Copper Created on CP Titanium Grade 2 by Plasma Electrolytic Oxidation

Krzysztof Rokosz [1,*], Tadeusz Hryniewicz [1], Wojciech Kacalak [1], Katarzyna Tandecka [1], Steinar Raaen [2], Sofia Gaiaschi [3], Patrick Chapon [3], Winfried Malorny [4], Dalibor Matýsek [5], Łukasz Dudek [1] and Kornel Pietrzak [1]

[1] Department of Engineering and Informatics Systems, Faculty of Mechanical Engineering, Koszalin University of Technology, Racławicka 15-17, PL 75-620 Koszalin, Poland; tadeusz.hryniewicz@tu.koszalin.pl (T.H.); wojciech.kacalak@tu.koszalin.pl (W.K.); katarzyna.tandecka@tu.koszalin.pl (K.T.); lukasz.dudek@tu.koszalin.pl (Ł.D.); kornel.pietrzak@s.tu.koszalin.pl (K.P.)

[2] Department of Physics, Norwegian University of Science and Technology (NTNU), Realfagbygget E3-124 Høgskoleringen 5, NO 7491 Trondheim, Norway; steinar.raaen@ntnu.no

[3] HORIBA FRANCE S.A.S., Avenue de la Vauve—Passage Jobin Yvon, CS 45002, 91120 Palaiseau, France; sofia.gaiaschi@horiba.com (S.G.); patrick.chapon@horiba.com (P.C.)

[4] Hochschule Wismar-University of Applied Sciences Technology, Business and Design, Faculty of Engineering, DE 23966 Wismar, Germany; winfried.malorny@hs-wismar.de

[5] Institute of Geological Engineering, Faculty of Mining and Geology, VŠB—Technical University of Ostrava, 708 33 Ostrava, Czech Republic; dalibor.matysek@vsb.cz

* Correspondence: rokosz@tu.koszalin.pl; Tel.: +48-94-3478354

Abstract: In the paper, the effect of voltage increase (from 500 V_{DC} up to 650 V_{DC}) on the structure and chemical composition of the porous coating on titanium made by Plasma Electrolytic Oxidation is presented. Phosphates-based coatings enriched with calcium, magnesium, zinc, and copper in electrolyte based on 1 L of 85% concentrated H_3PO_4, with additions of $Ca(NO_3)_2 \cdot 4H_2O$, and $Mg(NO_3)_2 \cdot 6H_2O$, and $Zn(NO_3)_2 \cdot 6H_2O$, and $Cu(NO_3)_2 \cdot 3H_2O$, are described. The morphology and chemical and phase composition are evaluated using SEM, EDS, XRD, XPS, GDOES, and CLSM. Based on these analyses, it was found that PEO coatings are porous and enriched with calcium, magnesium, zinc and copper. They consist mainly of the amorphous phase, which is more visible for higher voltages; this is correlated with an increase in the total PEO coating thickness (the higher the voltage, the thicker the PEO coating). However, for 650 V_{DC}, an amorphous phase and titanium substrate were also recorded, with a signal from $Ti_2P_2O_7$ crystalline that was not observed for lower voltages. It was also found that all obtained coatings may be divided into three sub-layers, i.e., porous, semiporous, and transitional.

Keywords: Plasma Electrolytic Oxidation (PEO); Micro Arc Oxidation (MAO); titanium

1. Introduction

The electrochemical treatment which is known in the literature as Plasma Electrolytic Oxidation (PEO), Micro Arc Oxidation (MAO), or Spark Discharge Anodizing (SDA) may be used to form micro-porous coatings on lightweight metals, such as titanium [1], zirconium [2], tantalum [3], niobium [4], and titanium alloys (Ti6Al4V [5], Ti6Al7Nb [6], Ti-Nb-Zr-Sn [7], NiTi [8], Ti13Nb13Zr [9].

The porous coatings obtained with such a method are mostly used as biomaterials, and are enriched with calcium and phosphorus to form a structure similar to that of hydroxyapatite [10], which may be doped by the addition of bactericidal copper [11], as well as zinc [12] and magnesium [13], added in case of acceleration of wound healing. The PEO processes may be performed under DC [7], AC [14,15], and pulse regime [16,17], which yields coatings with different porosities and chemical compositions, and also with different coating thicknesses. In the case of titanium and its alloys, the electrolytes which are used are mostly aqueous solutions with additions of various salts, acids and hydroxides, as presented in Table 1.

Table 1. Examples of aqueous electrolytes used to PEO (Plasma Electrolytic Oxidation) treatment of titanium and its alloys.

Electrolytes	Ref.
sodium silicate (Na_2SiO_3) with trisodium phosphate (Na_3PO_4), and sodium aluminate ($NaAlO_2$)	[5]
calcium hypophosphite $Ca(H_2PO_2)_2$ with phosphoric acid H_3PO_4	[9]
sodium phosphate monobasic monohydrate ($NaH_2PO_4 \cdot H_2O$) with calcium acetate hydrate ($Ca(CH_3COO)_2 \cdot H_2O$) and strontium hydroxide 8-hydrate ($Sr(OH)_2 \cdot 8H_2O$)	[18]
calcium acetate $Ca(CH_3COO)_2$ $2H_2O$, and Na_2SiO_3, ethylenediaminetetraacetic acid (EDTA), and sodium hydroxide NaOH	[19]
tri-sodium orthophosphate ($Na_3PO_4 \cdot 12H_2O$) with potassium hydroxide (KOH) and di-sodium tetra borate ($Na_2B_4O_7 \cdot 10H_2O$), and trisodium citrate dihydrate ($C_6H_5Na_3O_7 \cdot 2H_2O$), and sodium meta silicate nonahydrate ($Na_2SiO_3 \cdot 9H2O$)	[20]
disodium phosphate (Na_2HPO_4)	[21]
ammonium sulfate solution (($NH_4)_2SO_4$)	[22]
sodium dihydrogen phosphate (NaH_2PO_4) with calcium acetate ($Ca(CH_3COO)_2$) and strontium(II) acetate ($Sr(CH_3COO)_2$)	[23]
sodium hydroxide (NaOH) with sodium phytate ($Na_{12}Phy$)	[24]
sodium phosphate heptahydrate ($Na_2HPO_4 \cdot 7H_2O$), with α-Al_2O_3 and ketoconazole	[25]
trisodium phosphate (Na_3PO_4) with hydrated sodium borate ($Na_2B_4O_7$), and sodium tungstate ($Na_2WO_{4)}$	[26]
ethylenediaminetetraacetic acid (EDTA) with calcium ($Ca(CH_3COO)_2$), $Ca(H_2PO_4)_2$, sodium hydroxide (NaOH)	[27]

It should be pointed out that, in the majority of the literature, the presence of titanium oxides in PEO coatings obtained on titanium in aqueous solutions is most often reported. However, Sowa et. al. [9] reported that it was also possible to obtain a PEO coating in aqueous solution, in which mostly phosphates were detected. In the present paper, the continuation of previous works [13], i.e., the characterization of PEO coatings formed in electrolytes containing the concentrated phosphoric acid (H_3PO_4) with the addition of four nitrates ($Ca(NO_3)_2 \cdot 4H_2O$, $Mg(NO_3)_2 \cdot 6H_2O$, $Zn(NO_3)_2 \cdot 6H_2O$, $Cu(NO_3)_2 \cdot 3H_2O$), will be presented. The studies already carried out by the authors have shown that it is possible to obtain porous PEO coatings which are enriched only with copper [28] or calcium [29]. In addition, in reference to [13], new coatings obtained in electrolyte contacting two nitrates ($Zn(NO_3)_2 \cdot 6H_2O$, $Mg(NO_3)_2 \cdot 6H_2O$) were presented. It was found that their Zn/P and Mg/P ratios depend on the PEO voltage, and that the Zn/P ratio increases linearly with voltage; in contrast, the Mg/P ratio it is a constant function. That information led the authors to consider the possibility of creating new porous coatings enriched in more than two elements, and of determining the relation between elements originating from electrolyte (Ca, Cu, Mg, Zn, P). However, it was not possible to predict the composition of that coating based on the chemical composition of the electrolyte without experimental studies. Moreover, in the available literature there was no information on how such a porous coating would look, nor what its chemical composition would be, or the relation between each element. Therefore, the main goal of this paper is to present the results related to new porous PEO

coatings on titanium, which may be used as a transition layer between titanium biomaterial and tissue, as well as a porous substrate for catalysts. It should be also noted that the selection of elements, such as calcium, phosphorus, magnesium, zinc, and copper for new biocompatible coatings is based upon the need to create a hydroxyapatite-like structure ($Ca_5(PO_4)_3(OH)$), in which the Ca^{2+} ions can be replaced by antibacterial zinc Zn^{2+} and copper Cu^{2+} ions and by Mg^{2+} ions, which improve the healing of wounds. All the elements should be built into the porous structure in its entire volume; this will allow a slow release of selected ions into the body after surgery. On the other hand it should be pointed out that the obtained coatings, with developed surface stereometry, may be used for catalyst creation.

2. Materials and Methods

Titanium samples with dimensions of 10 mm $\times$ 10 mm $\times$ 2 mm were treated by Plasma Electrolytic Oxidation, at voltages of 500 V_{DC}, 575 V_{DC} and 650 V_{DC}, with the use of a commercial DC power supply (PWR 1600H, KIKUSUI Electronics Corporation, Yokohama, Japan). The electrolyte composition was the following: 1 L of 85% H_3PO_4, 125 g $Ca(NO_3)_2 \cdot 4H_2O$, 125 g $Mg(NO_3)_2 \cdot 6H_2O$, 125 g $Zn(NO_3)_2 \cdot 6H_2O$, and 125 g $Cu(NO_3)_2 \cdot 3H_2O$. The surface morphology was recorded by a scanning electron microscope (SEM) Quanta 250 FEI (Field Electron and Iron Company, Hillsboro, OR, USA) as well as an Energy-dispersive X-ray spectroscopy (EDS) (EDS Silicon Drift Detectors: Keith Thompson, Thermo Fisher Scientific, Madison, WI, USA). The depth profiles of PEO coatings were performed by Glow Discharge Optical Emission Spectroscopy (GDOES) [30] measurements, using a Horiba Scientific GD Profiler 2 instrument (HORIBA Scientific, Palaiseau, France) using a radio frequency (RF) pulsed source (700 Pa, 40 W, 3000 Hz) with an anode diameter of 4 mm (analyzed surface area equal to 12.56 mm^2). The structure was studied by Powder X-ray diffraction (XRD) using a Bruker-AXS D8 Advance instrument (BRUKER Corporation, Billerica, MA, USA), with the 2θ/θ geometry using a LynxEye position-sensitive detector (radiation CuKα/Ni filter, 40 kV, 40 mA, 0.014 2θ, interval of 0.25 s, BRUKER Corporation, Billerica, MA, USA). The quantitative and qualitative chemical compositions of the top 10 nm of PEO coatings were studied by X-ray photoelectron spectroscopy (XPS); measurements were made using SCIENCE SES 2002 instrument (SCIENTA AB, ScientaOmicron, Uppsala, Sweden) with a monochromatic (Gammadata-Scienta) Al K(alpha) ($h\nu$ = 1486.6 eV) X-ray source (18.7 mA, 13.02 kV). All studies were carried out on a surface of about 3 mm^2, with a pass energy of 500 eV (energy step 0.2 eV and step time 200 ms) with a base pressure of about $6 \cdot 10^{-8}$ Pa. The XPS spectra were processed in CasaXPS sotware [31] and interpreted based on NIST X-ray Photoelectron Spectroscopy Database [32] and XPS handbook [33]. SEM, EDS, XPS and GDOES measurement techniques, which have been used to characterize the PEO coatings, are described in detail in the references [13]. The surface topography of PEO coatings was evaluated by confocal laser scanning microscopy (CLSM), using a LEXT OLS4000 3D Laser Confocal Microscope (Olympus, Japan). A measuring field of 244 μm $\times$ 244 μm was scanned in three places on the surface coating. To obtain the measuring field, 4 scans were taken and then combined. Surface roughness was presented in 3D surface images. The following 3D parameters were calculated to obtain surface roughness: (*Sa*, *Sz*) (ISO 25178), where *Sa* it is arithmetical mean height (mean surface roughness), and *Sz* it is maximum height (height between the highest peak and the deepest valley). For statistical data processing, the descriptive statistics (mean, standard deviation, first quartile, third quartile), and rank score test at the level of significance α = 0.05, were used.

3. Results and Discussion

In Figure 1, the SEM images of porous coatings obtained on CP Titanium Grade 2 after PEO treatment at voltages of 500 V_{DC}, 575 V_{DC} and 650 V_{DC}, are presented. It can be observed that the voltage increase results in a change in surface morphology, as well as pore shapes and sharpness. Due to the fact that, on the basis of SEM images, it was not possible to differentiate the surfaces of the obtained PEO coatings, 3D roughness parameters were used to describe them, and are presented in Table 2.

Table 2. Statistical descriptions of 3D roughness parameters (*Sa* and *Sz*) in micrometers.

3D Roughness Parameter	Voltage	Mean	Stand. Dev.	First Quartile	Third Quartile
Sa	500 V$_{DC}$	1.74	0.29	1.44	2.02
	575 V$_{DC}$	2.08	0.15	1.92	2.22
	650 V$_{DC}$	3.50	0.06	3.45	3.57
Sz	500 V$_{DC}$	31.61	8.39	24.24	40.75
	575 V$_{DC}$	25.33	2.72	22.20	27.15
	650 V$_{DC}$	47.25	1.03	46.18	48.25

Based on parameters *Sa* (arithmetical mean height) and *Sz* (height between the highest peak and the deepest valley), it was possible to conclude that the smallest roughness was found for PEO coatings obtained at 500 V$_{DC}$ (*Sa* = 1.74 ± 0.29 μm, *Sz* = 31.61 ± 8.39 μm) and 575 V$_{DC}$ (*Sa* = 2.08 ± 0.15 μm, *Sz* = 25.33 ± 2.72 μm). By increasing the PEO voltage to 650 V$_{DC}$, it was noted that the two parameters, *Sa* and *Sz*, increased by about 50% relative to those ones associated with PEO coatings formed at 500 V$_{DC}$, and equal to *Sa* = 3.50 ± 0.06 μm, *Sz* = 47.25 ± 1.03 μm, respectively. It should be noted that the quantitative description by 3D roughness parameters (*Sa* and *Sz*) matches the SEM images presented in Figure 1. The external porosity, which may be described by those parameters, indicates that the larger the pore diameter, the higher the roughness parameters. Based on that notion, it may be concluded that coatings obtained at 500 V$_{DC}$ and 575 V$_{DC}$ have similar porosity; this was confirmed by a statistical rank score test at the level of significance α = 0.05, while those formed at 650 V$_{DC}$ have more open, volcanoes-like pores which are very clearly visible at the smallest magnification (500×) in Figure 1, and were confirmed by the same test.
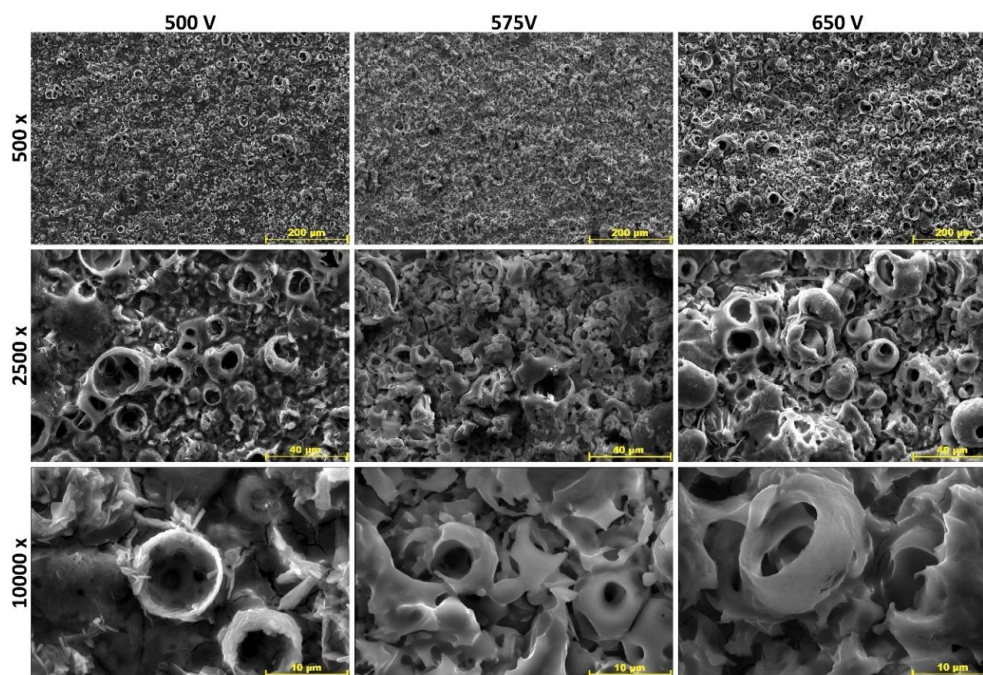
Figure 1. SEM images of coatings formed on Titanium after PEO process at voltages 500 V$_{DC}$, 575 V$_{DC}$, 650 V$_{DC}$ in 1 L of 85% H$_3$PO$_4$ with additions of 125 Ca(NO$_3$)$_2$·4H$_2$O, 125 g Mg(NO$_3$)$_2$·6H$_2$O, 125 g Zn(NO$_3$)$_2$·6H$_2$O, and 125 g Cu(NO$_3$)$_2$·3H$_2$O at magnifications 500, 1000, 2500, 5000, and 10000 times.

On the basis of EDS spectra, recorded at 500× magnification, the atomic concentrations of Ca, Mg, Zn, Cu, and P were used to calculate metals-to-phosphorus atomic ratios, with the results presented in Figure 2 and Table 3. Based on these results, it can be observed that Mg/P, Zn/P, Cu/P, and M/P

values have a positive correlation with voltage. The case of Ca/P values to voltage relation indicates the different mechanisms of calcium compounds in the layer. Considering the standard deviation values of the metal-to-phosphorus ratio, it can be concluded that the most repeatable conditions of the PEO process are at around 575 V_{DC}.

Table 3. Statistical descriptions of Ca/P, Mg/P, Zn/P, Cu/P, M/P ratios based on atomic percent (M = Ca + Mg + Zn + Cu).

| Ratios	Voltage	Mean	Stand. Dev.	First quartile	Third Quartile
Ca/P	500 V_{DC}	0.070	0.009	0.062	0.079
	575 V_{DC}	0.054	0.002	0.053	0.056
	650 V_{DC}	0.089	0.011	0.077	0.098
Mg/P	500 V_{DC}	0.037	0.002	0.035	0.038
	575 V_{DC}	0.044	0.002	0.042	0.046
	650 V_{DC}	0.045	0.001	0.043	0.046
Zn/P	500 V_{DC}	0.034	0.006	0.029	0.039
	575 V_{DC}	0.045	0.003	0.042	0.049
	650 V_{DC}	0.048	0.005	0.043	0.052
Cu/P	500 V_{DC}	0.032	0.002	0.030	0.033
	575 V_{DC}	0.037	0.003	0.033	0.040
	650 V_{DC}	0.043	0.011	0.036	0.052
M/P	500 V_{DC}	0.172	0.012	0.162	0.184
	575 V_{DC}	0.180	0.005	0.178	0.184
	650 V_{DC}	0.224	0.014	0.215	0.236
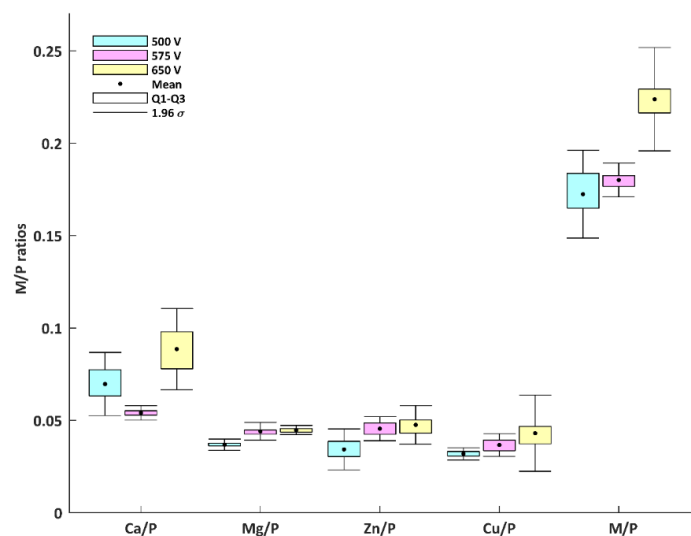
Figure 2. EDS results as Ca/P, Mg/P, Zn/P, Cu/P and M/P (M = Ca + Mg + Zn + Cu) ratios measured for coatings formed on CP Titanium Grade 2 after PEO process at the voltages 500 V_{DC}, 575 V_{DC}, 650 V_{DC} in 1 L of 85% H_3PO_4 with additions of 125 $Ca(NO_3)_2 \cdot 4H_2O$, 125 g $Mg(NO_3)_2 \cdot 6H_2O$, 125 g $Zn(NO_3)_2 \cdot 6H_2O$, and 125 g $Cu(NO_3)_2 \cdot 3H_2O$.

In Figure 3, the XPS spectra of PEO coating formed on Titanium at 575 V_{DC} are presented. Based on the registered peaks, it can be concluded that the top 10 nm layer of the PEO coating is enriched with calcium, magnesium, zinc, copper, and titanium, as well as phosphorus, oxygen, and nitrogen. It should be also pointed out that carbon bound with oxygen, as well as the nitrogen-oxygen compounds, should be treated as organic contaminants, which mainly originate from the air or from cleaning. The binding energies of 134.4 eV (P 2p) and 531.2 eV (O 1s) may be interpreted as PO_4^{3-}, or/and HPO_4^{2-}, or/and

$H_2PO_4^-$ or/and $P_2O_7^{4-}$ groups. The Cu 2p spectra with two main maxima (347.9 eV, 351 eV), as well as the satellite peaks existing in the range from 939 eV up to 947 eV as well as 566.8 eV (Cu LMM), may be interpreted as Cu^+ and Cu^{2+}, while the presence of Ca^{2+} is demonstrated by the binding energies which are equal to 347.9 eV and 351.4 eV. The binding energies at 497.9 eV (Zn LMM), 500.4 eV (Zn LMM), and 1022.4 eV (Zn 2p) may suggest the presence of Zn^{2+} in the PEO coating, whereas those equal to 50.6 eV (Mg 2p), 89.3 eV (Mg 2s), 306.8 eV (Mg KLL), indicate the presence of Mg^{2+}. The biding energy of titanium Ti $2p_{3/2}$ is shifted to 460.4 eV. This can be interpreted as a sign of the presence of Ti^{4+} in chemical compounds within Ca^{2+}, Zn^{2+}, Mg^{2+}, Cu^{2+}, and PO_4^{3-}, or/and HPO_4^{2-}, or/and $H_2PO_4^-$ or/and $P_2O_7^{4-}$. Based on quantitative analysis, it may be concluded that in the top 10 nm of PEO coatings, Ca:Mg:Zn:Cu ratios are equal to 16:29:1:1, 2:14:1:1, 6:17:1:1 for 500 V_{DC}, 575 V_{DC}, 650 V_{DC}, respectively. Based on these results, it may be concluded that the probability of calcium and magnesium incorporation into the structure is the highest, while for zinc and copper, the smallest, remaining constant in the function of voltage. The analysis of Ca/P, Mg/P, Zn/P, Cu/P, Ti/P, and M/P ratios allows us to conclude that a voltage increase, from 500 V_{DC} up to 650 V_{DC}, results in an increase in the Ca/P (from 0.033 up to 0.059) and Ti/P (from 0.051 up to 0.119) ratios, while for other ratios, i.e., Mg/P, Zn/P, Cu/P, and M/P, the maxima equaling 0.251, 0.018, 0.018, and 0.322, respectively, for 575 V_{DC}, were determined. Considering the fact that the amount of copper and zinc compounds in coating structure should be high enough to have antibacterial properties in the case of surgical treatment, it should be suitable for use in anodic oxidation, with a voltage of 575 V_{DC}.

Figures 4 and 5 present the GDOES profile of calcium, copper, magnesium, zinc, and phosphorus, oxygen, hydrogen, and titanium, respectively, for PEO coatings. Based on these results, it is possible to conclude that the PEO coatings may be described by a three-sub-layer model. The first porous and top sub-layers are enriched with phosphorus, oxygen, calcium, copper, magnesium, and zinc. However, it should be noted that the maxima of signals in that sub-layer may be partly related to plasma inflammation and organic contaminations from the air or/and cleaning process. These are mainly registered for phosphorus (178 nm), as well as oxygen (130 nm) and hydrogen (122 nm) signals, which may be a part of structure (coating matrix) containing the phosphates and hydrogen phosphates enriched in calcium, magnesium, zinc, and copper, whose signals are much weaker in this range. In the second sub-layer, which is semiporous with nested finer pores in the pores, a plateau was observed for all GDOES signals. In that sublayer, the amount of chemical components originating from the electrolyte (calcium, magnesium, zinc, and copper) are stable; this is especially important in the case of biomaterials, because the possibility of tissue growing into the porosity of PEO coating during healing after surgery. It should therefore be protected from bacteria, which is associated with copper and zinc ions. In addition, calcium and phosphorus form the hydroxyapatite-like structure, which should be acceptable for tissue, and magnesium as an accelerator of wound healing. In places in the GDOES signals, where local maxima of calcium, copper, magnesium, zinc, and phosphorus are observed, the third transition sub-layer, in which increasing the levels of titanium and decreasing those of phosphorus, oxygen, calcium, copper, magnesium, and zinc are observed, has its beginning. Moreover, maxima in the hydrogen signals, which are in the middle of this sub-layer, should be treated as the end of the porosity of the coating. Based on the GDOES spectra, one can infer that an increase in the PEO voltage results in an increase of the coating thickness, which may be expressed in sputtering times in seconds. Therefore, all the sublayer thicknesses depend on PEO voltage. The top one has thicknesses of 200 s, 300 s, and 400 s of sputtering time for 500 V_{DC}, 575 V_{DC}, 650 V_{DC}, respectively, while the thickness of the second one is in the range of 1200 s (500 V_{DC}) up to 2900 s (650 V_{DC}) of sputtering time. For the thickness of the third, the transition layer increases with an increase in voltage from 1100 s (500 V_{DC}) up to 2000 s (650 V_{DC}) of sputtering time. In addition, it was observed that the thickness of the first sub-layer may be described by a linear trend in function of PEO voltage, i.e., 1.33 U-66.67, while the second and the third ones follow the equations: 11.33 U-4550 and 6 U-1950, respectively, where U is in the range from 500 V_{DC} to 650 V_{DC}.
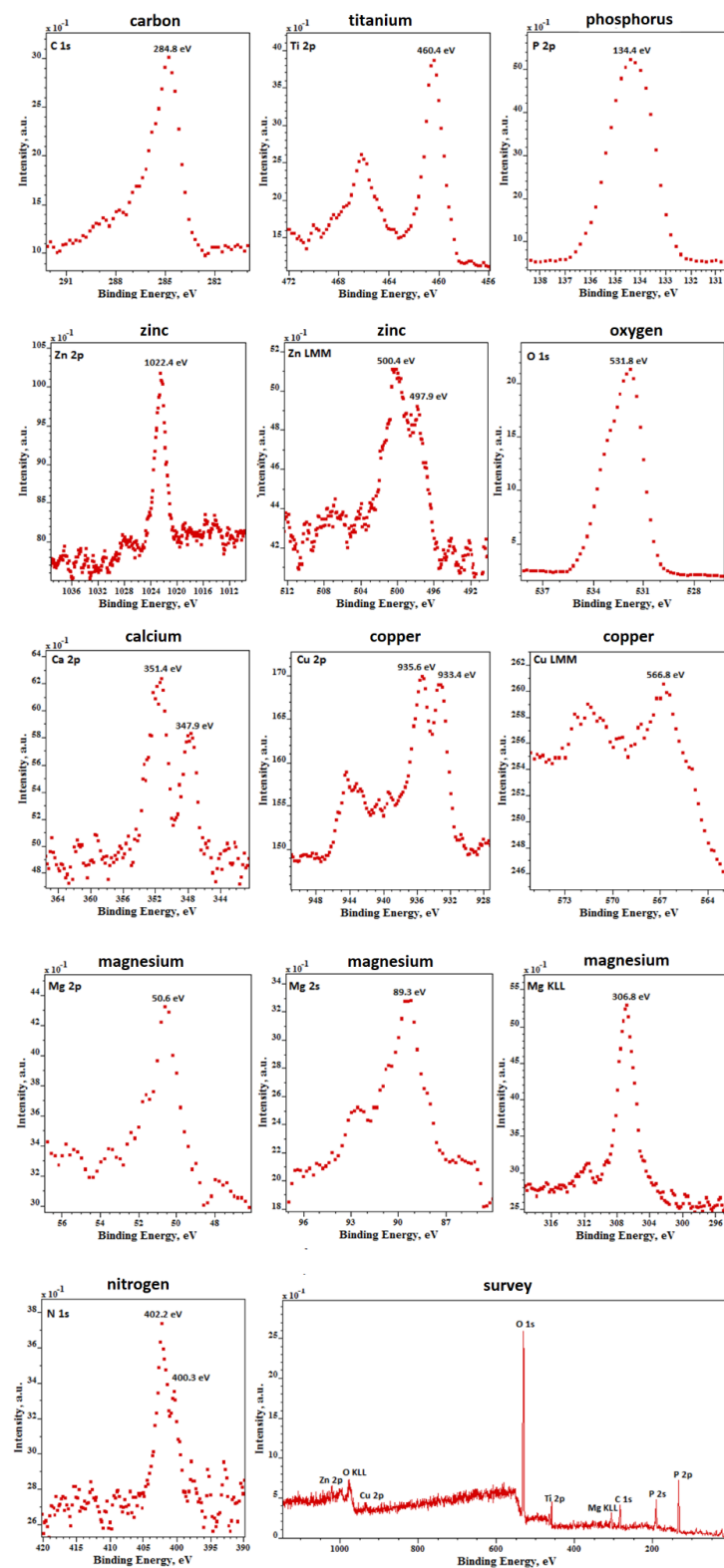
Figure 3. XPS spectra of coatings formed on CP Titanium Grade 2 after PEO process at voltage 575 V_{DC} in 1 L of 85% H_3PO_4 with additions of 125 g $Ca(NO_3)_2 \cdot 4H_2O$, 125 g $Mg(NO_3)_2 \cdot 6H_2O$, 125 g $Zn(NO_3)_2 \cdot 6H_2O$, and 125 g $Cu(NO_3)_2 \cdot 3H_2O$.
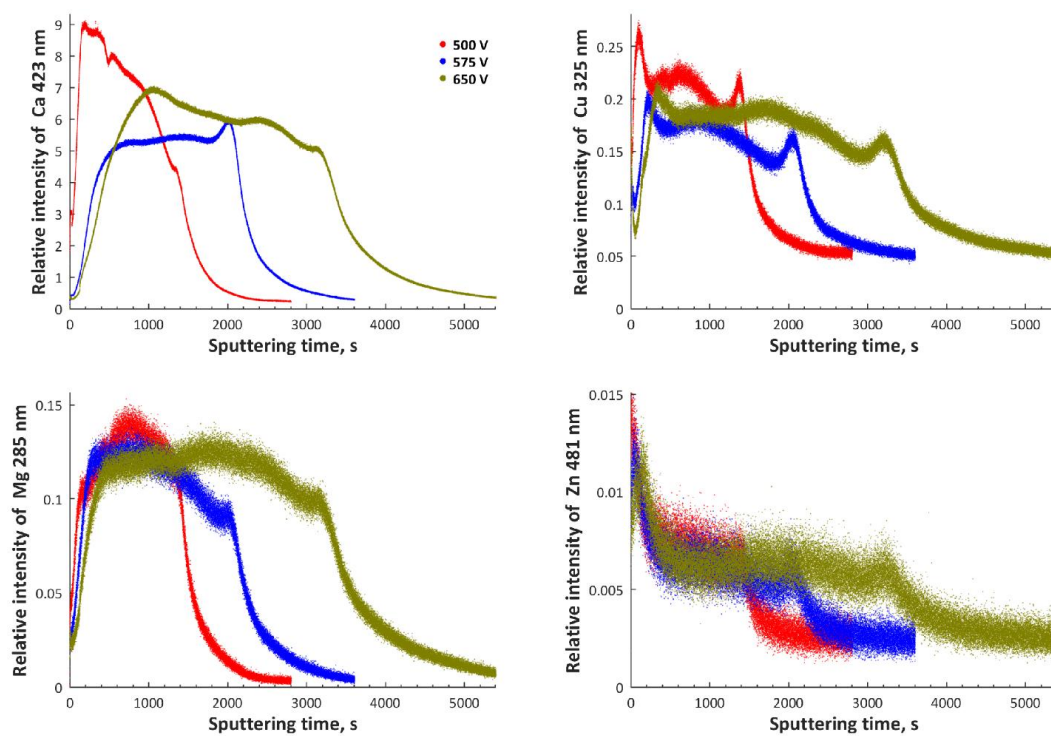
Figure 4. GDEOS (Glow Discharge Optical Emission Spectroscopy) signals of calcium (Ca), magnesium (Mg), copper (Cu) and zinc (Zn) of coatings formed on CP Titanium Grade 2 after PEO process at voltages 500 V_{DC}, 575 V_{DC}, 650 V_{DC}, in 1 L of 85% H_3PO_4 with the additions of 125 g $Ca(NO_3)_2 \cdot 4H_2O$, 125 g $Mg(NO_3)_2 \cdot 6H_2O$, 125 g $Zn(NO_3)_2 \cdot 6H_2O$, and 125 g $Cu(NO_3)_2 \cdot 3H_2O$.
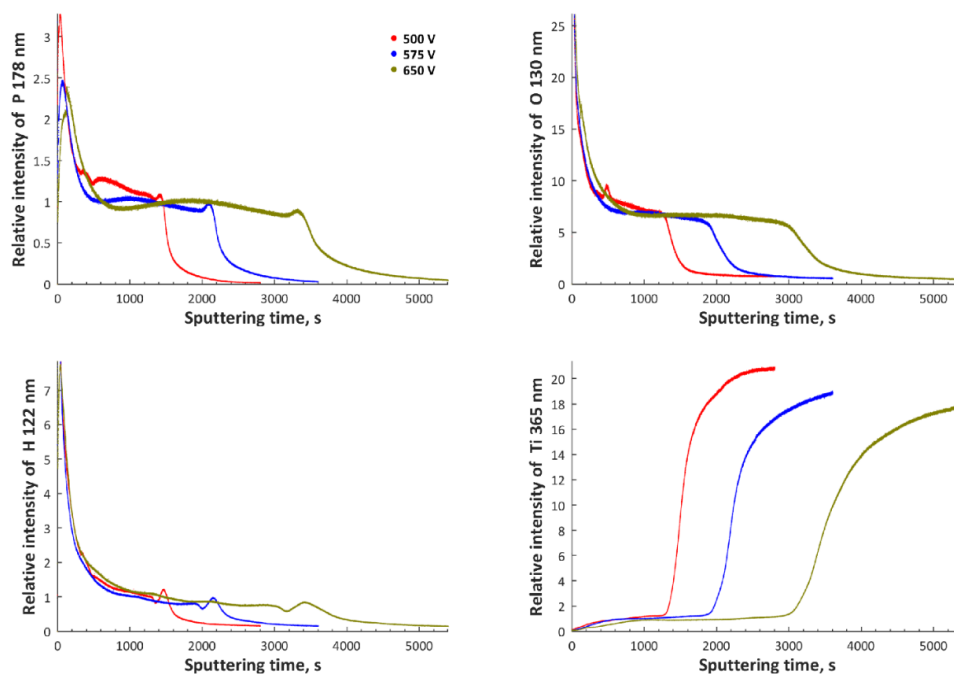
Figure 5. GDEOS signals of phosphorus (P), oxygen (O), hydrogen (H) and titanium (Ti) of coatings formed on CP Titanium Grade 2 after PEO process at voltages 500 V_{DC}, 575 V_{DC}, 650 V_{DC}, in 1 L of 85% H_3PO_4 with the additions of 125 g $Ca(NO_3)_2 \cdot 4H_2O$, 125 g $Mg(NO_3)_2 \cdot 6H_2O$, 125 g $Zn(NO_3)_2 \cdot 6H_2O$, and 125 g $Cu(NO_3)_2 \cdot 3H_2O$.

The phase composition of the PEO samples was studied by XRD, and the results are presented in Figure 6. These results show that, beyond the titanium signal coming from the substrate, the amorphous layer can be also identified. It should be pointed out that the higher the voltage, the higher the amorphous phase; this is due to an increase in the coating thickness. However, in the case of the PEO coating obtained at 650 V_{DC}, in addition to the amorphous phase, diffraction peaks due to the presence of $Ti_2P_2O_7$ crystals, can be observed.
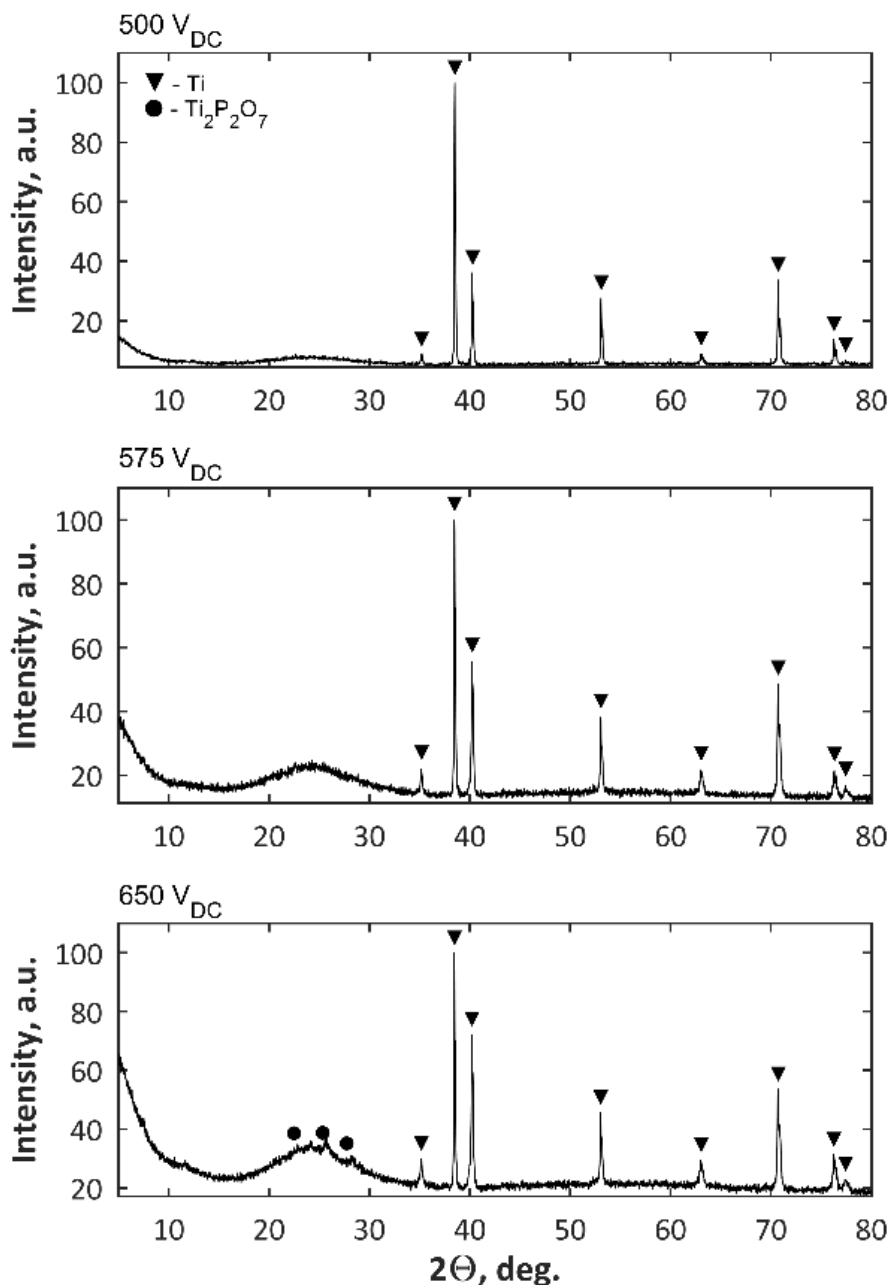
Figure 6. XRD (X-ray Diffraction) patterns of coatings formed on CP Titanium Grade 2 after PEO process at voltages 500 V_{DC}, 575 V_{DC}, 650 V_{DC}, in 1 L of 85% H_3PO_4 with the additions of 125 g $Ca(NO_3)_2 \cdot 4H_2O$, 125 g $Mg(NO_3)_2 \cdot 6H_2O$, 125 g $Zn(NO_3)_2 \cdot 6H_2O$, and 125 g $Cu(NO_3)_2 \cdot 3H_2O$.

4. Summary

These studies allowed us to conclude that voltages ranging from 500 V_{DC} to 650 V_{DC} result in the formation of porous coatings enriched with phosphorus, oxygen, calcium, copper, magnesium,

and zinc on titanium after the Plasma Electrolytic Oxidation process. It should be pointed out that, for the first time, the new electrolyte containing 85% concentrated phosphoric acid (H_3PO_4) with the addition of calcium nitrate $Ca(NO_3)_2 \cdot 4H_2O$, magnesium nitrate $Mg(NO_3)_2 \cdot 6H_2O$, zinc nitrate $Zn(NO_3)_2 \cdot 6H_2O$, and copper nitrate $Cu(NO_3)_2 \cdot 3H_2O$, was used by the authors. It was observed that the external porosity of the obtained coatings may be described by 3D roughness parameters, such as the arithmetical mean height (*Sa*) and maximum height (*Sz*). Between the surfaces of the PEO coating obtained at voltages of 500 V_{DC} and 575 V_{DC}, there is no significant difference among the 3D roughness parameters; this was confirmed by a statistical rank score test at the level of significance $\alpha = 0.05$, while that formed at 650 V_{DC} shows a different porosity, which was confirmed by the same statistical test. The chemical composition studies, based on EDS measurements, have shown that with increasing PEO voltage, the metal-to-phosphorus ratios also increase, while the XPS studies of the top 10 nm of PEO coatings show that the maximum of that ratio (0.332) was recorded at 575 V_{DC}. It should be noted that the chemical composition is not the same in the whole volume of these coatings. In addition, the top 10 nm of porous coatings are most likely composed of titanium (Ti^{4+}), calcium (Ca^{2+}), magnesium (Mg^{2+}), zinc (Zn^{2+}), copper (Cu^{2+} and Cu^+), and phosphates (PO_4^{3-} and/or HPO_4^{2-}, and/or $H_2PO_4^-$, and/or $P_2O_7^{4-}$). It should be also pointed out that, in the obtained structure of PEO coatings for one zinc atom or one copper atom, which are bactericidal, there may be up to 16 calcium and 29 magnesium atoms, as it was observed in the coatings formed at voltage 575 V_{DC}. Based on the GDOES and XRD studies, it was found that the higher voltage, the thicker the PEO coating, i.e., the thickest coating may be obtained at 650 V_{DC} and the thinnest at 500 V_{DC}, which is more amorphous with a crystalline phase $Ti_2P_2O_7$. The three sub-layer model for PEO coating description was used, i.e., the authors proposed the following three sublayers: the top, porous one (contaminated with carbon-nitrogen-oxygen compounds originating from the air and cleaning process), the second, semiporous one (enriched in phosphorus, oxygen, calcium, copper, magnesium, and zinc, and depleted in titanium), and a transition one (increasing the amount of titanium, with decreasing amounts of phosphorus, oxygen, calcium, copper, magnesium, and zinc). In summary, it should be noted that the obtained porous coatings, which are enriched in selected elements such as calcium, phosphorus, magnesium, and bactericidal copper and zinc, can be used to increase the biocompatibility of titanium biomaterials, as well as for the creation of new substrates for catalysts with highly developed surface stereometries.

Author Contributions: K.R. and T.H. conceived and designed the experiments; K.R., S.G., P.C., S.R., D.M., K.T., and W.M. performed the experiments; K.R., T.H., W.K., K.T., Ł.D., and K.P. analyzed the data; K.R., T.H., Ł.D. and K.P. contributed reagents, materials, analysis tools; K.R. and T.H. wrote the paper.

Conflicts of Interest: The authors declare no conflict of interest.

References

1. Wang, Y.; Jiang, B.; Lei, T.; Guo, L. Dependence of growth features of microarc oxidation coatings of titanium alloy on control modes of alternate pulse. *Mater. Lett.* **2004**, *58*, 1907–1911. [CrossRef]

2. Sowa, M.; Lastowka, D.; Kukharenko, A.I.; Korotin, D.M.; Kurmaev, E.Z.; Cholakh, S.O.; Simka, W. Characterisation of anodic oxide films on zirconium formed in sulphuric acid: XPS and corrosion resistance investigations. *J. Solid State Electrochem.* **2017**, *21*, 203–210. [CrossRef]

3. Sowa, M.; Kazek-Kęsik, A.; Socha, R.P.; Dercz, G.; Michalska, J.; Simka, W. Modification of tantalum surface via plasma electrolytic oxidation in silicate solutions. *Electrochim. Acta* **2013**, *114*, 627–636. [CrossRef]

4. Pereira, B.L.; Lepienski, C.M.; Mazzaro, I.; Kuromoto, N.K. Apatite grown in niobium by two-step plasma electrolytic oxidation. *Mater. Sci. Eng. C Mater. Biol. Appl.* **2017**, *77*, 1235–1241. [CrossRef] [PubMed]

5. Korkmaz, K. The effect of Micro-arc Oxidation treatment on the microstructure and properties of open cell Ti6Al4V alloy foams. *Surf. Coat. Technol.* **2015**, *272*, 72–78. [CrossRef]

6. Simka, W.; Nawrat, G.; Chlode, J.; Maciej, A.; Winiarski, A.; Szade, J.; Radwanski, K.; Gazdowicz, J. Electropolishing and anodic passivation of Ti6Al7Nb alloy. *Przem. Chem.* **2011**, *90*, 84–90.

7. Rokosz, K.; Hryniewicz, T.; Raaen, S.; Chapon, P. Investigation of porous coatings obtained on Ti-Nb-Zr-Sn alloy biomaterial by Plasma Electrolytic Oxidation: Characterisation and Modelling. *Int. J. Adv. Manuf. Technol.* **2016**, *87*, 3497–3512. [CrossRef]

8. Siu, H.T.; Man, H.C. Fabrication of bioactive titania coating on nitinol by plasma electrolytic oxidation. *Appl. Surf. Sci.* **2014**, *274*, 181–187. [CrossRef]

9. Sowa, M.; Piotrowska, M.; Widziołek, M.; Dercz, G.; Tylko, G.; Gorewoda, T.; Osyczka, A.M.; Simka, W. Bioactivity of coatings formed on Ti13Nb13Zr alloy using plasma electrolytic oxidation. *Mater. Sci. Eng. C* **2015**, *49*, 159–173. [CrossRef] [PubMed]

10. Simka, W.; Sadowski, A.; Warczak, M.; Iwaniak, A.; Dercz, G.; Michalska, J.; Maciej, A. Modification of titanium oxide layer by calcium and phosphorus. *Electrochim. Acta* **2011**, *56*, 8962–8968. [CrossRef]

11. Villapún, V.M.; Dover, L.G.; Cross, A.; González, S. Antibacterial Metallic Touch Surfaces. *Materials* **2016**, *9*, 736. [CrossRef] [PubMed]

12. Jansson, T.; Clare-Salzler, Z.J.; Zaveri, T.D.; Mehta, S.; Dolgova, N.V.; Chu, B.H.; Ren, F.; Keselowsky, B.G. Antibacterial effects of zinc oxide nanorod surfaces. *J. Nanosci. Nanotechnol.* **2012**, *12*, 7132–7138. [CrossRef] [PubMed]

13. Rokosz, K.; Hryniewicz, T.; Gaiaschi, S.; Chapon, P.; Raaen, S.; Pietrzak, K.; Malorny, W.; Fernandes, J.S. Characterization of Porous Phosphate Coatings Enriched with Magnesium or Zinc on CP Titanium Grade 2 under DC Plasma Electrolytic Oxidation. *Metals* **2018**, *8*, 112. [CrossRef]

14. Aliasghari, S.; Němcová, A.; Skeldon, P.; Thompson, G.E. Influence of coating morphology on adhesive bonding of titanium pre-treated by plasma electrolytic oxidation. *Surf. Coat. Technol.* **2016**, *289*, 101–109. [CrossRef]

15. Gnedenkov, S.V.; Sharkeev, Y.P.; Sinebryukhov, S.L.; Khrisanfova, O.A.; Legostaeva, E.V.; Zavidnaya, A.G.; Puz', A.V.; Khlusov, I.A.; Opra, D.P. Functional coatings formed on the titanium and magnesium alloys as implant materials by plasma electrolytic oxidation technology: Fundamental principles and synthesis conditions. *Corros. Rev.* **2016**, *34*, 65–83. [CrossRef]

16. Hariprasad, S.; Ashfaq, M.; Arunnellaiappan, T.; Harilal, M.; Rameshbabu, N. Role of electrolyte additives on in-vitro corrosion behavior of DC plasma electrolytic oxidization coatings formed on CP-Ti. *Surf. Coat. Technol.* **2016**, *292*, 20–29.

17. Huang, Q.; Elkhooly, T.A.; Liu, X.; Zhang, R.; Yang, X.; Shen, Z.; Feng, Q. Effects of hierarchical micro/nano-topographies on the morphology, proliferation and differentiation of osteoblast-like cells. *Colloid Surf. B Biointerfaces* **2016**, *145*, 37–45. [CrossRef] [PubMed]

18. Kung, K.C.; Yuan, K.; Lee, T.M.; Lui, T.S. Effect of heat treatment on microstructures and mechanical behavior of porous SrCaP coatings on titanium. *J. Alloy. Compd.* **2012**, *515*, 68–73. [CrossRef]

19. Zhou, R.; Wei, D.; Cheng, S.; Zhou, Y.; Jia, D.; Wang, Y.; Li, B. The effect of titanium bead diameter of porous titanium on the formation of micro-arc oxidized TiO2-based coatings containing Si and Ca. *Ceram. Int.* **2013**, *39*, 5725–5732. [CrossRef]

20. Venkateswarlu, K.; Rameshbabu, N.; Sreekanth, D.; Sandhyarani, M.; Bose, A.; Muthupandi, V.; Subramanian, S. Role of electrolyte chemistry on electronic and in vitro electrochemical properties of micro-arc oxidized titania films on Cp Ti. *Electrochim. Acta* **2013**, *105*, 468–480.

21. Çelik, İ.; Alsaran, A.; Purcek, G. Effect of different surface oxidation treatments on structural, mechanical and tribological properties of ultrafine-grained titanium. *Surf. Coat. Technol.* **2014**, *258*, 842–848. [CrossRef]

22. Komiya, S.; Sakamoto, K.; Ohtsu, N. Structural changes of anodic layer on titanium in sulfate solution as a function of anodization duration in constant current mode. *Appl. Surf. Sci.* **2014**, *296*, 163–168. [CrossRef]

23. Liu, W.; Cheng, M.; Wahafu, T.; Zhao, Y.; Qin, H.; Wang, J.; Zhang, X.; Wang, L. The in vitro and in vivo performance of a strontium-containing coating on the low-modulus Ti35Nb2Ta3Zr alloy formed by micro-arc oxidation. *J. Mater. Sci. Mater. M* **2015**, *26*, 1–13. [CrossRef] [PubMed]

24. Zhang, R.F.; Qiao, L.P.; Qu, B.; Zhang, S.F.; Chang, W.H.; Xiang, J.H. Biocompatibility of micro-arc oxidation coatings developed on Ti6Al4V alloy in a solution containing organic phosphate. *Mater. Lett.* **2015**, *153*, 77–80. [CrossRef]

25. Sharifi, H.; Aliofkhazraei, M.; Darband, G.B.; Rouhaghdam, A.S. Tribological properties of PEO nanocomposite coatings on titanium formed in electrolyte containing ketoconazole. *Tribol. Int.* **2016**, *102*, 463–471. [CrossRef]

26. Koblova, E.A.; Ustinov, A.Y.; Rudnev, V.S.; Lukiyanchuk, I.V.; Chernykh, I.V. An X-ray photoelectron spectroscopy study of Ni, Cu-containing coatings formed by plasma electrolytic oxidation on aluminum and titanium. *J. Struct. Chem.* **2017**, *58*, 1129–1136. [CrossRef]

27. Wang, L.; Erasquin, U.J.; Zhao, M.; Ren, L.; Zhang, M.Y.; Cheng, G.J.; Wang, Y.; Cai, C. Stability, Antimicrobial Activity, and Cytotoxicity of Poly(amidoamine) Dendrimers on Titanium Substrates. *ACS Appl. Mater. Interfaces* **2011**, *3*, 2885–2894. [CrossRef] [PubMed]

28. Rokosz, K.; Hryniewicz, T.; Matysek, D.; Raaen, S.; Valíček, J.; Dudek, Ł.; Harničarova, M. SEM, EDS and XPS analysis of the coatings obtained on titanium after plasma electrolytic oxidation in electrolytes containing copper nitrate. *Materials* **2016**, *9*, 318. [CrossRef] [PubMed]

29. Rokosz, K.; Hryniewicz, T.; Gaiaschi, S.; Chapon, P.; Raaen, S.; Pietrzak, K.; Malorny, W. Characterisation of calcium- and phosphorus-enriched porous coatings on CP Titanium Grade 2 fabricated by plasma electrolytic oxidation. *Metals* **2017**, *7*, 354. [CrossRef]

30. Nelis, T.; Payling, R. *Practical Guide to Glow Discharge Optical Emission Spectroscopy*; RSC Analytical Spectroscopy Monographs; Barnett, N.W., Ed.; Royal Society of Chemistry: Cambridge, UK, 2002.

31. Casa Software Ltd. CasaXPS: Processing Software for XPS, AES, SIMS and More. 2009. Available online: http://www.casaxps.com (accessed on 24 May 2018).

32. Naumkin, A.V.; Kraut-Vass, A.; Gaarenstroom, S.W.; Powell, C.J. NIST X-ray Photoelectron Spectroscopy Database: NIST Standard Reference Database 20, Version 4.1. 2012. Available online: https://srdata.nist.gov/xps/ (accessed on 24 May 2018).

33. Moulder, J.F.; Stickle, W.F.; Sobol, P.E.; Bomben, K.D. *Handbook of X-ray Photoelectron Spectroscopy*; Chastain, J., Ed.; Perkin-Elmer Corporation: Eden Prairie, MN, USA, 1992.